FURTHER APPLICATIONS OF CYCLIC VOLTAMMETRY WITH SPHERICAL ELECTRODES

Marién M. Moreno[1] and Angela Molina[2,*]

Departamento de Química Física, Facultad de Química, Universidad de Murcia, Espinardo, Murcia 30100, Spain; e-mail: [1] mencarna@um.es, [2] amolina@um.es

Received May 21, 2004
Accepted July 28, 2004

In this work we show analytical and easily manageable explicit equations corresponding to the application of any multipulse potential sequence to planar, spherical and cylindrical electrodes. We apply these expressions to study reversible charge transfer electrode processes in cyclic voltammetry with spherical electrodes, by considering that both members of the redox pair are initially present in solution, and showing that a conventional symmetrical sweep can be used under these conditions. These expressions allow study in depth fundamental aspects of cyclic voltammetry with spherical electrodes. Thus, in the cyclic voltammograms obtained for simple reversible processes with conventional spherical electrodes at different sweep rates, characteristic common points of non zero current (isopoints) appear from which unknown thermodynamic parameters of these systems can be easily determined. From these equations it can be predicted and demonstrated that there are important analogies of the *I/E* behavior between a simple reversible charge transfer reaction and a first-order catalytic process when any single or multipulse voltammetric transient techniques are applied.

Keywords: Cyclic voltammetry; Spherical electrodes; Catalytic mechanism; Multipulse potential sequence; Reversible charge transfer processes; Electrochemistry.

In this paper we present explicit and easily manageable equations corresponding to a reversible charge transfer process (E_r) based on previous results[1,2]. These equations are applicable to planar, spherical and cylindrical electrodes and show that the current corresponding to any multipulse technique can be expressed as the sum of formally identical summands which contain two factors, one dependent only on time and electrode geometry, and the other dependent only on the surface concentrations. It is important to highlight that this behavior is exclusive for E_r processes[2], multistep reversible processes[3] and first-order catalytic mechanism (E_rC')[4,5]. This is because in all these cases the surface concentrations are independent of time and are only dependent on the potential of the actual pulse applied in planar, spherical, and cylindrical geometries.

We will apply these equations to the study of the most commonly used multipulse technique, cyclic voltammetry (CV), in the most general situation in which both members of the redox pair are initially present in solution, by using the usual symmetrical sweep instead of the awkward asymmetrical sweep beginning at the equilibrium potential[6–8]. Our equations reveal that when conventional-size spherical electrodes are used in CV or cyclic staircase voltammetry (CSCV) techniques, the *I/E* curves obtained for different sweep rates present one or two common points (isopoints) of non zero current, depending on whether one or both electroactive species are present in solution. The presence of these isopoints is of great interest in establishing completely the fundaments of CV technique, in order to describe the ideal behavior of an E_r process in spherical diffusion. However, these points have never been characterized in the literature due, undoubtedly, to the absence of analytical explicit equations.

The above theoretical predictions have been experimentally verified for an E_r process with the ferrioxalate system in a static mercury dropping electrode (SMDE), and with solutions containing both members of the redox pair $Fe(CN)_6^{3-}/Fe(CN)_6^{4-}$ at a planar electrode.

We have also compared the analytical expressions corresponding to voltammetric behavior of the E_r and E_rC' mechanism, which indicate clearly that both mechanisms present important analogies in transient techniques. This is due to the fact that of all reaction mechanisms with first-order chemical reactions coupled to a reversible charge transfer reaction (i.e., E_rC, CE_r, E_rCE_r, CE_rC, E_rC', ...), the E_rC' mechanism[4,5] is the only one for which the expression of the current corresponding to any transient multipulse technique presents an analytical form comparable to that shown for the E_r mechanism analyzed in this paper, independently of the value of the equilibrium and rate constants of the homogeneous chemical reaction.

EXPERIMENTAL

A computer-driven potentiostat-galvanostat was designed and constructed by QUICELTRON (Spain). Pulse and waveform generation and data acquisition were performed using i-SBXDD4 and DAS16-330i (ComputerBoards, U.S.A.) boards, respectively. All computer programs were written in our laboratory.

A three-electrode cell was employed in the experiments. A static mercury dropping electrode and a Pt planar disk (r_0 = 0.25 cm) served as working electrodes. The SMDE was constructed using a dropping mercury electrode EA 1019-1 (Metrohm) to which a home-made valve was sealed. The electrode radius of the SMDE was determined by weighing a large number of drops. The counter electrode was a Pt foil and the reference was a Ag|AgCl|KCl 1.0 M electrode.

All reagents were of Merck analytical grade and were used without further purification. Working solutions containing $Fe(C_2O_4)_3^{3-}$ were freshly prepared in order to avoid error from photochemical reduction. Water was bidistilled and nitrogen gas was used for deaeration. In all the experiments the temperature was kept constant at 25 ± 0.2 °C.

For the experimental curves shown in Fig. 2, the background current has been corrected and the diffusion coefficient value used in theoretical adjustment, $D = (4.6 \pm 0.1) \times 10^{-6}$ cm^2/s, was previously obtained from chronoamperometric experiments.

REVERSIBLE CHARGE TRANSFER REACTION (E_r)

Let us consider a reversible charge transfer process, E_r, when both oxidized and reduced species, O and R, may be initially present in the electrolytic solution with concentrations c_O^* and c_R^*, respectively.

For these conditions, it is possible to apply a general treatment for the multipotential problem, with any value of diffusion coefficients in planar diffusion ($D_O \neq D_R$), and taking $D_A = D_B$ in spherical and cylindrical diffusion, based on the fact that for all the above cases, the surface concentrations, $c_{O,s}^p$ and $c_{R,s}^p$, corresponding to the application of an arbitrary sequence of consecutive potential steps, (designed by $E_{in} = E_1, E_2, \ldots, E_{p-1}, E_p$), are only dependent on the potential applied in the last step, E_p, and hence are independent of the previous history of the system[1].

In this case, by generalizing the results of previous papers and by applying the superposition principle[1,2], the current corresponding to the p-th pulse for a planar electrode whose area increases with an arbitrary power of time, $A(t) = A_0 t^z$, or for spherical and even for cylindrical electrodes, can be written in this general and elegant form

$$I^p = nFA\left(\frac{D_O}{\pi}\right)^{1/2}\left\{\sum_{m=1}^{p} F_{E_r}(t_{mp})\left(c_{O,s}^{m-1} - c_{O,s}^{m}\right)\right\} \quad p = 1, 2, \ldots, \qquad (1)$$

which contains p summands that are the product of two factors: (i) a function dependent on time and on the electrode geometry, $F(t_{mp})$, and (ii) the difference between surface concentrations of consecutive potential steps, $c_{O,s}^{m-1} - c_{O,s}^{m}$, depending only on the potential as indicated in Table I.

The surface concentrations corresponding to any p-th pulse, $c_{O,s}^p$ and $c_{R,s}^p$, are only dependent on the actual pulse potential applied, independently of the diffusion field considered, and are given by

$$c_{O,s}^p = \frac{K_p(\gamma c_O^* + c_R^*)}{1 + \gamma K_p} \quad p = 1, 2, \ldots \qquad (2)$$

TABLE I

Analytical expressions for $F_{E_r}(t_{mp})$ and $c_{O,s}^{m-1} - c_{O,s}^{m}$ (see Eq. (*1*)) corresponding to a reversible charge transfer reaction for different electrode geometries. For cylindrical electrodes (Eqs (*4*) and (*5*) in this table), $y = Dt_{mp}/r_0^2$ and $\gamma_E = 0.577216$ (Euler constant)

Diffusion	Area	$F_{E_r}(t_{mp})$		$c_{O,s}^{m-1} - c_{O,s}^{m}$	
Planar $D_O \neq D_R$	Increasing with an arbitrary power of time $A_0 t_{1p}^{z}$	$\sqrt{\dfrac{(2z+1)}{t_{1p}\left[1-\left(1-\dfrac{t_{mp}}{t_{1p}}\right)\right]^{(2z+1)}}}$	(*1*)	$\left(\dfrac{1}{1+\gamma K_m} - \dfrac{1}{1+\gamma K_{m-1}}\right)\dfrac{(\gamma c_O^* + c_R^*)}{\gamma}$ $K_0 = c_O^* / c_R^*$ $\gamma = \left(\dfrac{D_O}{D_R}\right)^{1/2}$	(*6*)
	Static A_0	$\dfrac{1}{(t_{mp})^{1/2}}$	(*2*)		
Spherical $D_O = D_R$	$4\pi r_0^2$	$\dfrac{1}{(t_{mp})^{1/2}} + \dfrac{(\pi D)^{1/2}}{r_0}$	(*3*)		
Cylindrical $D_O = D_R$	$2\pi rl$	$\dfrac{(\pi D)^{1/2}}{r_0}\left\{\dfrac{1}{(\pi y)^{1/2}} + 0.422 + 0.0675 \log y + \right.$ $\left. + 0.0058 \operatorname{sgn}[\log y - 1.47][\log y - 1.47]^2\right\}$ for $y < 1200$	(*4*)	$\left(\dfrac{1}{1+K_m} - \dfrac{1}{1+K_{m-1}}\right)(c_O^* + c_R^*)$ $K_0 = c_O^* / c_R^*$	(*7*)
		$\dfrac{(\pi D)^{1/2}}{r_0}\left\{\dfrac{2}{\ln(4y) - 2\gamma_E} - \dfrac{2\gamma_E}{[\ln(4y) - 2\gamma_E]^2} - \right.$ $\left. - \dfrac{2.624}{[\ln(4y) - 2\gamma_E]^3} + \dfrac{1.033}{[\ln(4y) - 2\gamma_E]^4} + \ldots\right\}$ for $y \geq 1200$	(*5*)		

and

$$c_{\mathrm{R,s}}^{p} = \frac{\gamma c_{\mathrm{O}}^{*} + c_{\mathrm{R}}^{*}}{1 + \gamma K_p} \tag{3}$$

for an expanding or static planar electrode, with

$$\gamma = \left(\frac{D_{\mathrm{O}}}{D_{\mathrm{R}}} \right)^{1/2} \tag{4}$$

and

$$c_{\mathrm{O,s}}^{p} = \frac{K_p (c_{\mathrm{O}}^{*} + c_{\mathrm{R}}^{*})}{1 + K_p} \quad p = 1, 2, \ldots \tag{5}$$

$$c_{\mathrm{R,s}}^{p} = \frac{c_{\mathrm{O}}^{*} + c_{\mathrm{R}}^{*}}{1 + K_p} \tag{6}$$

for spherical or cylindrical electrodes when $D_{\mathrm{O}} = D_{\mathrm{R}} = D$, with

$$K_p = \exp\left(\frac{nF(E_p - E^{0\prime})}{RT} \right) \quad p = 1, 2, \ldots . \tag{7}$$

Moreover, for $m = 1$ in Eq. (*1*), $c_{\mathrm{O,s}}^{m-1} = c_{\mathrm{O,s}}^{0} = c_{\mathrm{O}}^{*}$ correspond to the initial concentrations ($K_0 = c_{\mathrm{O}}^{*}/c_{\mathrm{R}}^{*}$ depends on equilibrium potential $E_{\mathrm{eq}} = E_0 = E^{0\prime} + RT \ln (c_{\mathrm{O}}^{*}/c_{\mathrm{R}}^{*})/nF$), and the time, t_{mp}, is that elapsed between the beginning of the application of the m-th potential step and the end of the application of the p-th potential step

$$t_{mp} = \sum_{q=m}^{p} t_q \ , \tag{8}$$

where t_q is the duration of any potential step, E_q.

From these equations it is possible to obtain the expression for the current corresponding to any multipulse electrochemical technique, e.g., staircase voltammetry (SCV), cyclic staircase voltammetry, linear sweep voltammetry (LSV) and cyclic voltammetry. In this work we study the responses corresponding to spherical electrodes of any radius, r_0, including planar ($r_0 \to \infty$) and ultramicrospherical ($r_0 \to 0$) electrodes.

Cyclic Voltammetry

To apply the above equations to the multipulse techniques CSCV or CV we must take into account that the applied perturbation *E/t* consists of a cyclic stepped potential or a cyclic linear sweep potential, respectively. All the potential steps have the same duration, $t_1 = t_2 = ... = \tau$, and the same pulse amplitude, $|\Delta E| = E^{p+1} - E^p$, with the scan being applied between the initial potential, $E_{in} = E_1$, and the reversal potential, E_r, at which the direction sweep is changed.

Thus, the classical dimensionless current is studied in the form[9]

$$\psi = \frac{I^p}{nFA(c_O^* + c_R^*)(aD)^{1/2}} , \qquad (9)$$

where I^p is the current at the end of the *p*-th step (see Eq. (*1*)) and the potential sweep rate is defined as[9]

$$a = \frac{nF}{RT}\nu = \frac{nF}{RT}\frac{|\Delta E|}{\tau} . \qquad (10)$$

By introducing Eqs (*9*)–(*10*) into Eq. (*1*), along with the $F_{E_r}(t_{mp})$ function given by Eq. (*3*) in Table I, we deduce the dimensionless current in CSCV and CV for spherical electrodes when both species are initially in solution

$$\psi = \frac{1}{(c_O^* + c_R^*)(\pi a\tau)^{1/2}} \sum_{m=1}^{p} \left(\frac{1}{(p-m+1)^{1/2}} + \frac{(\pi D\tau)^{1/2}}{r_0} \right) \left(c_{O,s}^{m-1} - c_{O,s}^{m} \right) . \qquad (11)$$

This equation can be used in cyclic voltammetry by introducing the condition $|\Delta E| \to 0$. In general, very good results are obtained for values of $|\Delta E| < 0.01$ mV [1,5]. Under these conditions, the term containing the dependence with the potential applied, $c_{O,s}^{m-1} - c_{O,s}^{m}$ in Eq. (*11*), fulfils (see Eq. (*7*))

$$\frac{-\mathrm{d}c_{O,s}^{m}}{\mathrm{d}E_j} = \lim_{|\Delta E| \to 0^{\mp}} \frac{\left(c_{O,s}^{m-1} - c_{O,s}^{m} \right)}{|\Delta E|} = \pm \frac{nF}{RT} \frac{K_m}{(1+K_m)^2} , \qquad (12)$$

where the double sign refers to the direction sweep, with the upper sign corresponding to the cathodic sweep ($\Delta E < 0$) and the lower sign to the anodic one ($\Delta E > 0$). Thus, by using the above mathematical identity in

Eq. (*11*), it is possible to write in a new and more elegant form the current obtained for reversible processes at spherical electrodes of any size

$$\psi = \psi^{\text{planar}} + \psi^{\text{radial}} \tag{13}$$

with

$$\psi^{\text{planar}} = \frac{1}{(\pi a t)^{1/2}} \frac{c_O^* - K_1 c_R^*}{(c_O^* + c_R^*)(1 + K_1)} \pm \left(\frac{a\tau}{\pi}\right)^{1/2} \sum_{j=2}^{p} \frac{1}{(p - j + 1)^{1/2}} \frac{K_j}{(1 + K_j)^2} , \tag{14}$$

where t is the duration of experiment and

$$\psi^{\text{radial}} = \frac{1}{(c_O^* + c_R^*) r_0} \left(\frac{D}{a}\right)^{1/2} \frac{c_O^* - K_p c_R^*}{(1 + K_p)} . \tag{15}$$

ψ (Eqs (*13*)–(*15*)) is a very easily programmable expression which is valid for any experimental conditions chosen, including any value of initial potential ($E_{in} = E_1$), since its influence on the current when both species O and R are initially in solution is clearly expressed by the first addend of Eq. (*14*).

Only One Species is Initially in the Solution

When only the oxidized species O is initially present ($c_R^* = 0$) and the scan starts at $E_{in} >> E^{0'}$ ($K_{in} = K_1 \to \infty$), the expression for planar contribution, ψ^{planar} (Eq. (*14*)) coincides, for $|\Delta E| < 10^{-2}$ mV , with the results calculated by several authors in planar diffusion[9,10]. The excellent approximation for the radial contribution, $\phi(\sigma t)$, given by Reinmuth in Eq. (*4*) of lit.[11], which was used by Nicholson and Shain[9], is only valid when there is no reduced species R initially present[12]. In such case, the results obtained are practically coincident with the ψ^{radial} given by Eq. (*15*) with $c_R^* = 0$. Therefore, as long as both species are initially present in the electrolytic solution, Eqs (*13*)–(*15*) of this paper need to be used to calculate the current at spherical electrodes of any radius, r_0.

In Fig. 1 we have plotted the cyclic voltammograms corresponding to an electrode of A =1.26 × 10^{-5} cm^2 by using three values for the potential sweep rate, v = 10^3, 10^2, and 10 mV/s . Figures 1a and 1b show the planar (I^{planar}, see Eqs (*9*) and (*14*)) and radial (I^{radial}, see Eqs (*9*) and (*15*)) contributions, respectively. Figure 1c corresponds to the real current that we would

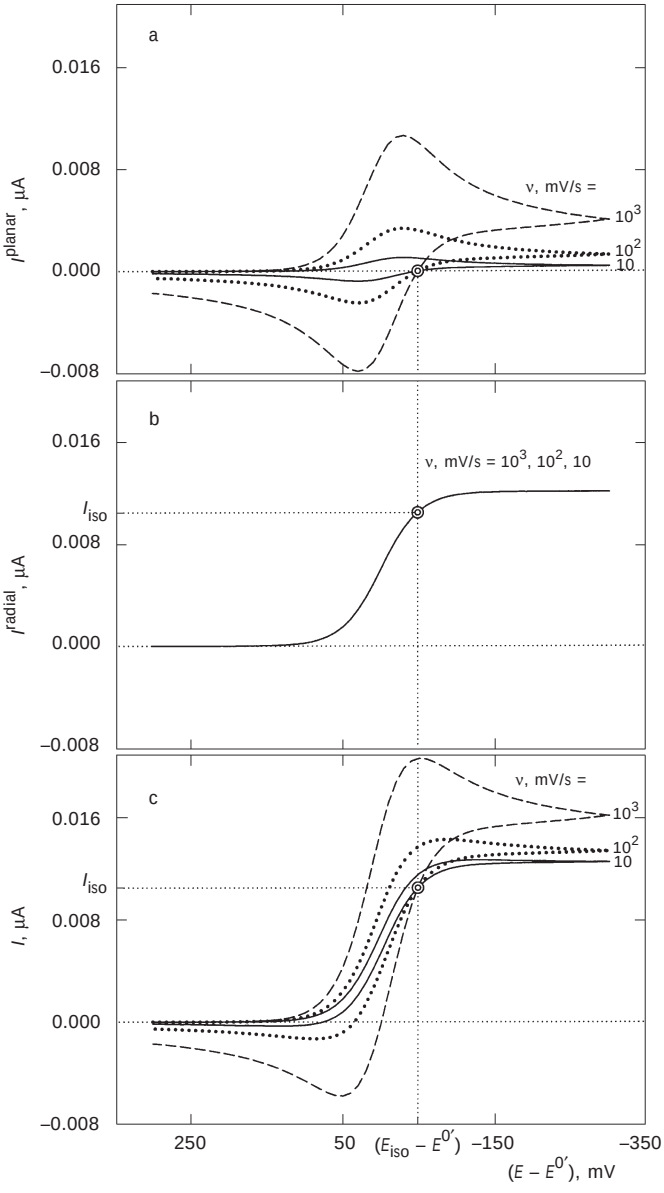

FIG. 1

$I/(E - E^{0'})$ curves for a reversible process in CV. a Planar contribution, Eqs (*9*) and (*14*); b radial contribution, Eqs (*9*) and (*15*); c spherical electrode, Eqs (*9*) and (*13*). $A = 1.26 \times 10^{-5}$ cm^2, $n = 1$, $D = 10^{-5}$ cm^2/s, $T = 298.15$ K, $c_R^* = 0$, $|\Delta E| = 0.01$ mV. The values of v (in mV/s) are given in the figure. The coordinates of the non zero current isopoint ($E_{iso} - E^{0'}$, I_{iso}) are shown in Fig. 1c

expect to obtain for a spherical electrode (I, see Eqs (*9*) and (*13*)). As can be seen, planar and spherical curves (Figs 1a and 1c), present a common point in the reverse branches of the *I/E* curves obtained at different sweep rate values. This point has been previously described in the literature for planar electrodes under the name of "isopoint", as a point of zero current observed for reversible kinetics[13] (Fig. 1a).

It can be easily demonstrated that the current corresponding to this point independent of sweep rate, is zero for planar electrodes, i.e., $I_{iso}^{planar} = I^{planar}(E_{iso}) = 0$ (see Eqs (*9*) and (*14*) and also lit.[13]). For spherical electrodes this isopoint also exists, but it corresponds to a non zero cathodic current which is due solely to the radial contribution which is independent of the sweep rate (see Fig. 1b), i.e., $I_{iso} = I^{radial}(E_{iso})$. In this case, the expression of I_{iso} can be easily calculated by making $I_{iso}^{planar} = 0$. So, we deduce (see Eqs (*9*) and (*15*))

$$I_{iso}(c_O^*) = \frac{nFADc_O^*}{r_0(1+K_{iso})}, \qquad (16)$$

where, in accordance with definition (*7*),

$$K_{iso} = \exp\left(\frac{nF(E_{iso} - E^{0'})}{RT}\right). \qquad (17)$$

Thus, when conventional spherical electrodes are used, the formal potential can be easily determined from the above expression being given by

$$E^{0'} = E_{iso} - \frac{RT}{nF}\ln\left(\frac{I_{d,O}(\infty) - I_{iso}(c_O^*)}{I_{iso}(c_O^*)}\right) \qquad (18)$$

with $I_{iso}(c_O^*)$ being the current measured at $E = E_{iso}$ and $I_{d,O}(\infty)$ is the hypothetical steady state diffusion cathodic limiting current for a sphere of any radius, given by[14]

$$I_{d,O}(\infty) = 4\pi nFDr_0c_O^* . \qquad (19)$$

To the best of our knowledge, this point has never been characterized in the literature when spherical electrodes are used. However, it is of great interest for establishing the basics of this technique since it confirms the ideal behavior of a reversible charge transfer process, together with the cathodic

peak potential, E_{pc}, the separation between cathodic and anodic peaks, ΔE_p, etc.

Figure 2 shows the experimental (dotted lines) and theoretical (solid lines) curves corresponding to CV with the system 1 mM $FeCl_3$ in 0.25 M $K_2C_2O_4$ and pH 4.70 ± 0.05. The experimental currents were obtained by applying several sweep rates to a spherical electrode of radius r_0 = 0.014 cm. The isopoint position has been determined by linear fitting of experimental data close to the intercept point. The average values are E_{iso} = –279 ± 1 mV and I_{iso} = 0.066 ± 0.001 μA , so the formal potential deduced by applying Eq. (*18*) is $E^{0'}$ = –235 ± 2 mV. The theoretical curves were constructed with the data $E^{0'}$ = –235 mV and $D = 4.6 \times 10^{-6}$ cm^2/s (see Experimental). Both values are in good agreement with those previously reported in the literature[15,16] and, as can be seen, the agreement between theoretical and experimental currents is very good.

The shape of the *I/E* curves obtained from the backward scan is affected by the reversal potential value, E_r, at which the direction sweep is changed[9,10,17]. Thus, the usual parameters related to the anodic sweep change with E_r – like the separation between peaks, $\Delta E_p = E_{pa} - E_{pc}$, and also the new characterized isopoint (E_{iso}, I_{iso}) – but the isopoint remains a single point even when reversal is made early. This isopoint of non zero current is a universal characteristic of CV and CSCV curves obtained for reversible

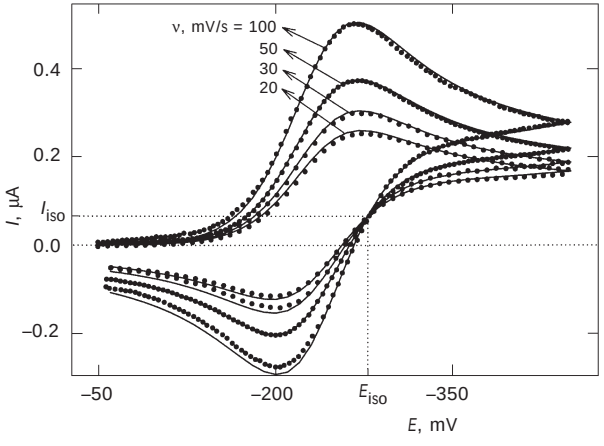

FIG. 2

Comparison between experimental (dotted lines) and theoretical (solid lines, Eqs (*9*) and (*13*)–(*15*)) cyclic voltammograms for 1 mM Fe^{3+} in 0.25 M $K_2C_2O_4$, pH 4.70 ± 0.05. r_0 = 0.014 cm, $D = 4.6 \times 10^{-6}$ cm^2/s, E_{iso} = –279 ± 1 mV, I_{iso} = 0.066 ± 0.001 μA. The values of *v* (in mV/s) are given in the figure. Other conditions as in Fig. 1

processes with spherical electrodes when the steady state has not been reached. The current corresponding to this point is given by Eq. (*16*) and therefore will be observable for any experimental conditions chosen, including any values of initial and reversal potential, E_{in} and E_r, as well as for any value of pulse amplitude, $|\Delta E|$. This isopoint can also be found in CSCV, and its current is also given by Eq. (*16*).

In Table II we have summarized the values of the isopotential, $E_{iso} - E^{0'}$, and the dimensionless isocurrent, $I_{iso}/I_{d,O}(\infty)$, calculated for CV technique by applying Eqs (*13*)–(*15*) with $c_R^* = 0$, for different reversal potential values, E_r, with spherical electrodes and the equivalent parameters with planar electrodes, $(E_{iso} - E^{0'})^{planar}$ and I_{iso}^{planar}, for comparison. Note that $E_{iso} - E^{0'}$ and $I_{iso}/I_{d,O}(\infty)$ are independent of electrode radius, r_0, and sweep rate values, v, and are only dependent on the reversal potential, E_r. Table II shows, as an example, the values obtained for the separation between anodic and cathodic peaks, ΔE_p, in a spherical electrode with $r_0 = 0.01$ cm, $v = 100$ mV/s and $D = 10^{-5}$ cm^2/s ($(D/r_0^2 a)^{1/2} = 0.1603$). In these conditions, the cathodic peak potential takes the value $E_{pc} - E^{0'} = -36.4$ mV ($(E_{pc} - E^{0'})^{planar} = -28.5$ mV for a planar electrode). ΔE_p decreases when the reversal potential, E_r, becomes more negative, in such a way that the anodic peak shifts towards anodic potentials, as occurs in planar diffusion[9,10,17]. When the radius de-

TABLE II

Influence of the reversal potential ($E_r - E^{0'}$) on the coordinates of isopoints ($E_{iso} - E^{0'}$, $I_{iso}/I_{d,O}(\infty)$) (Eqs (*23*)–(*25*) with $E_{in} - E^{0'} = -300$ mV and $|\Delta E| = 10^{-6}$ mV) and on the separation between peaks for a spherical electrode, ΔE_p, ($(D/r_0^2 a)^{1/2} = 0.1603$, $r_0 = 0.01$ cm, $v = 100$ mV/s) and for a planar electrode, ΔE_p^{planar}. The positions obtained for cathodic peaks are $E_{pc} - E^{0'} = -36.4$ mV and $(E_{pc} - E^{0'})^{planar} = -28.5$ mV. Others conditions as in Fig. 1

$E_r - E^{0'}$	$E_{iso} - E^{0'} = (E_{iso}^{planar} - E^{0'})$	$I_{iso}/I_d(\infty)$	I_{iso}^{planar}	ΔE_{peak}	ΔE_{peak}^{planar}
mV	mV			mV	mV
–100	–28.1	0.7488	0.0	76.2	60.2
–150	–36.5	0.8052	0.0	74.7	58.8
–200	–41.9	0.8363	0.0	74.0	58.2
–250	–45.9	0.8564	0.0	73.7	57.8
–300	–49.0	0.8707	0.0	73.5	57.6
–∞	–73.5	0.9459	0.0	72.8	57.1

These data have been calculated taking $|\Delta E| = 10^{-6}$ mV, although with $|\Delta E| = 10^{-2}$ mV relative errors of less than ±1% in the peak currents and deviations of less than ±0.5 mV in the peak potentials are found.

creases, the ΔE_p difference increases, except for ultramicroelectrodes for which both peaks disappear. Hence, ΔE_p always takes greater values for conventional spherical electrodes than for planar electrodes.

Influence of the Presence of Reaction Product

In the literature when both species are initially in solution, the CV technique has only been applied with planar electrodes in an unusual and unnecessary way, beginning the scan at the equilibrium potential $E_{in} = E_{eq}$ ($K_{in} = K_0$, Eq. (*7*))[6–8] and moving the potential applied towards cathodic or anodic values[7]. However, all equations given in this paper are general expressions which, as well as being valid for planar and spherical electrodes of any radius, including microelectrodes, can also be used for any value of initial potential, E_{in}, different from E_{eq}, i.e., for conditions of non zero initial current.

Figure 3 shows the cyclic voltammograms obtained for a spherical electrode of radius $r_0 = 0.01$ cm, when applying Eqs (*13*)–(*15*) with several values of the relation between initial concentrations of the redox pair, $c_R^*/(c_O^* + c_R^*)$. In Fig. 3a the cathodic sweep starts at $E_{in} = E_{eq}$ and continues up to $E_r = E_{eq} - 15RT/(nF)$, whereas the anodic sweep ends at a much more positive potential value than E_{eq} in such a way that the whole sweep is asymmetrical[7,8].

If the usual symmetric sweep starts at sufficient positive potentials ($E_{in} = (E^{0'} + 400)$ mV), the oxidation reaction takes place and an anodic current is obtained at the beginning of experiment, as is shown in the curves of Fig. 3b. This initial current value, ψ_{in}^a, can be easily deduced from Eqs (*13*)–(*15*). So, if $E_{in} >> E^{0'}$, ψ_{in}^a is given by

$$\psi_{in}^a = \frac{-c_R^*}{(c_O^* + c_R^*)} \left(\frac{RT}{nF|\Delta E|} \right)^{1/2} \left\{ \frac{1}{(\pi t)^{1/2}} + \frac{D^{1/2}}{r_0} \right\}. \qquad (20)$$

If the sweep starts at very negative potentials, $E_{in} << E^{0'}$, ψ_{in}^c takes the form

$$\psi_{in}^c = \frac{c_O^*}{(c_O^* + c_R^*)} \left(\frac{RT}{nF|\Delta E|} \right)^{1/2} \left\{ \frac{1}{(\pi t)^{1/2}} + \frac{D^{1/2}}{r_0} \right\}. \qquad (21)$$

Note that in these conditions the initial current in CV tends to minus infinity or to infinity at the beginning of the experiment, while in CSCV it takes a constant value[5]. As expected, in Figs 3a and 3b it can be observed

how the cathodic peak current diminishes and the anodic peak current increases when the ratio $c_R^*/(c_O^* + c_R^*)$ increases. This effect is more pronounced when the electrode radius decreases.

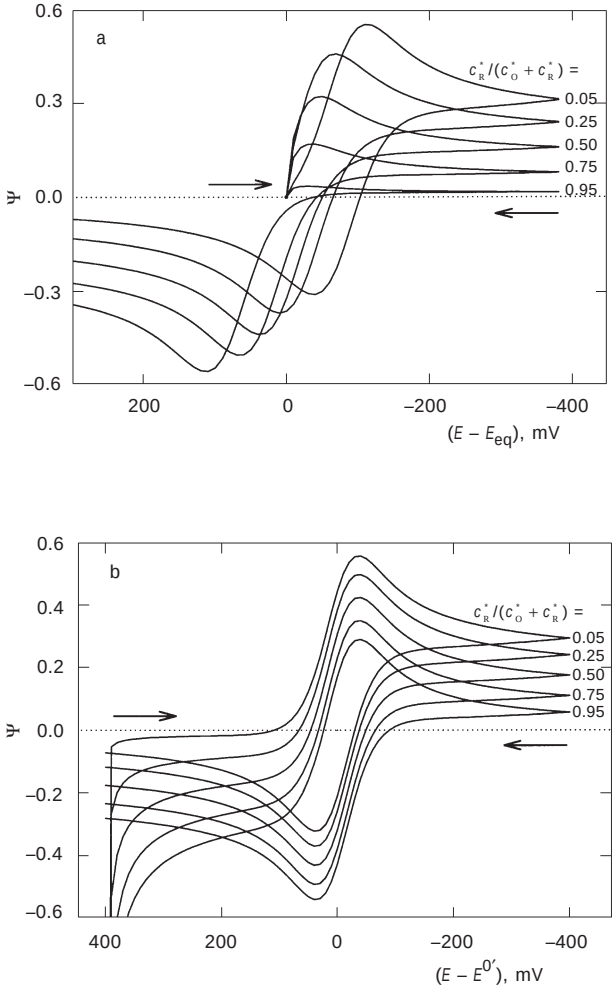

FIG. 3

Influence of $c_R^*/(c_O^* + c_R^*)$ on the dimensionless cyclic voltammograms for a spherical electrode, ψ_{CV} (Eqs (*13*)–(*15*)). a Asymmetrical sweep, $E_{in} = E_{eq}$, $E_r = E_{eq} - (15RT/nF)$; b symmetrical sweep, $E_{in} = (E^{0'} + 400)$ mV, $E_r = (E^{0'} - 400)$ mV. $r_0 = 0.01$ cm, $v = 100$ mV/s. The values of $c_R^*/(c_O^* + c_R^*)$ are given in the figure. Other conditions as in Fig. 1

Figure 4a shows the influence of sweep rate on the cyclic voltammograms obtained when both members of the redox pair are initially present with $c_O^* = c_R^*$ and beginning the scan in the negative direction from $E_{in} = E_{eq}$. As can be seen, an isopoint appears in the reversal branch of these curves, just as in the case described above when only species O is initially present. However, the relation between I_{iso} and E_{iso} is now given by

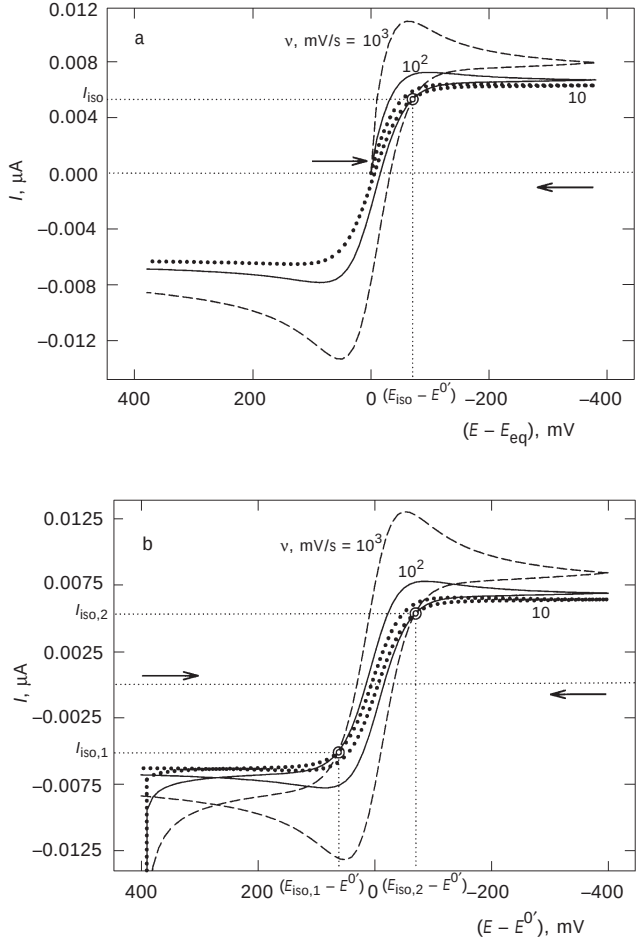

FIG. 4

Influence of sweep rate on the cyclic voltammograms for a spherical electrode, I_{CV} (Eqs (*9*) and (*13*)–(*15*)), when both species are initially present with $c_O^* = c_R^*$ ($c_B^*/c^* = 0.5$). a Asymmetrical sweep, one isopoint; b symmetrical sweep, two isopoints. The values of v (in mV/s) are given in the figure. Others conditions as in Fig. 6

$$I_{\mathrm{iso}} = \frac{nFAD}{r_0} \frac{c_{\mathrm{O}}^{*} - K_{\mathrm{iso}} c_{\mathrm{R}}^{*}}{1 + K_{\mathrm{iso}}} . \qquad (22)$$

In these conditions, we find for the formal potential the following expression

$$E^{0'} = E_{\mathrm{iso}} - \frac{RT}{nF} \ln \left(\frac{I_{\mathrm{d,O}}(\infty) - I_{\mathrm{iso}}}{I_{\mathrm{iso}} - I_{\mathrm{d,R}}(\infty)} \right), \qquad (23)$$

where $I_{\mathrm{d,O}}(\infty)$ corresponds to the limiting cathodic current given by Eq. (*21*) and $I_{\mathrm{d,R}}(\infty)$ is the limiting anodic current given by

$$I_{\mathrm{d,R}}(\infty) = -4\pi nFDr_0 c_{\mathrm{R}}^{*} . \qquad (24)$$

If E_{in} is very positive ($E_{\mathrm{in}} = (E_{\mathrm{eq}} + 400)$ mV in Fig. 4b), two intercept points (isopoints) of non zero currents are observed in spherical diffusion, ($E_{\mathrm{iso},1}$, $I_{\mathrm{iso},1}$) and ($E_{\mathrm{iso},2}$, $I_{\mathrm{iso},2}$). For each of these points Eq. (*22*) is fulfilled, so we can obtain, for example, $E^{0'}$ and D by applying any numerical method to solve this system of two equations.

Evidently, two isopoints, both with zero current, are also observed for planar diffusion. This behavior has been experimentally verified in Fig. 5. which shows the experimental voltammograms obtained with different

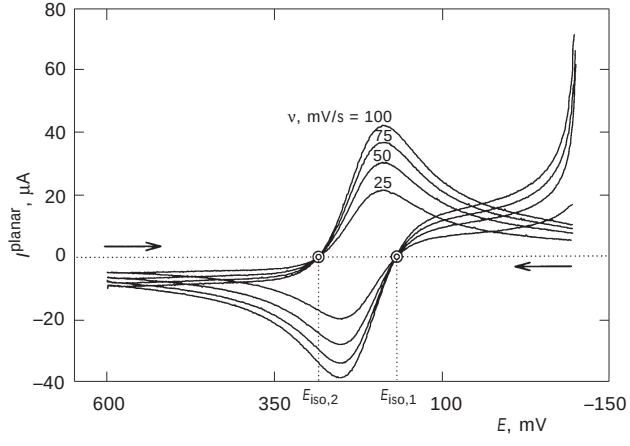

FIG. 5

Experimental cyclic voltammograms obtained for 0.5 mM $Fe(CN)_6^{3-}$/0.5 mM $Fe(CN)_6^{4-}$ in 0.5 M KCl with a Pt disk of r_0 = 0.25 cm. The isopoints have been localized at $E_{\mathrm{iso},1}$ = 167 ± 1 mV, $E_{\mathrm{iso},2}$ = 285 ± 1 mV, $I_{\mathrm{iso},1}^{\mathrm{planar}} = I_{\mathrm{iso},2}^{\mathrm{planar}} = 0.0$. The values of v (in mV/s) are given in the figure

sweep rates for the $Fe(CN)_6^{3-}/Fe(CN)_6^{4-}$ system when both species are initially in solution with equal concentrations, $c_O^* = c_R^* = 0.5$ mmol/l. The potential range at which this system is electroactive is incompatible with the use of a SMDE, so a large Pt disk electrode has been used in order to minimize edge effects, and two isopoints of zero current are observed. The symmetric scan was started at sufficiently positive potentials ($E_{in} = -100$ mV), so initial oxidation currents given by Eq. (*20*) are also observed.

FIRST-ORDER CATALYTIC MECHANISM (E_RC'). COMPARISON WITH A REVERSIBLE E PROCESS (E_r)

The simplest scheme for the E_rC' mechanism can be written by

$$O + n\,e^- \rightleftarrows R$$

$$R \underset{k_2}{\overset{k_1}{\rightleftarrows}} O$$

Of all the reaction mechanisms with first-order chemical reactions coupled to the reversible charge transfer reaction (i.e., E_rC, CE_r, E_rCE_r, CE_rC, E_rC', ...), E_rC' is the only mechanism that presents clear analogies with the E_r mechanism analyzed in this paper. These analogies are observed in voltammetric transient techniques for any value of the equilibrium and rate constant of the homogeneous chemical reaction. This behavior which, as far as we know, has not been discussed in depth in the literature, is due to the fact that the E_rC' mechanism is the only mechanism for which the surface concentrations of electroactive species are independent of time for any pulse potential applied, as has been recently shown in lit.[4,5]. This makes it possible to write for the current corresponding to any *p*-th pulse for the E_rC' mechanism in spherical diffusion in a mode formally similar to that corresponding to an E_r process (Eq. (*1*)). So, by a generalization of the results shown in lit.[4,5] for any *p*-th potential step we find

$$I^p_{E_rC'} = nFA\left(\frac{D_O}{\pi}\right)^{1/2} \sum_{m=1}^{p} F_{E_rC'}(t_{mp})\left(c^{m-1}_{O,s} - c^{m}_{O,s}\right), \qquad (25)$$

where

$$F_{E_rC'}(t_{mp}) = \frac{e^{-(k_1+k_2)t_{mp}}}{(t_{mp})^{1/2}} + \left[\pi(k_1+k_2)\right]^{1/2} \operatorname{erf}\left[(k_1+k_2)t_{mp}\right]^{1/2} + \frac{(\pi D)^{1/2}}{r_0} \qquad (26)$$

and $c_{O,s}^{m-1} - c_{O,s}^{m}$ has an identical form to that previously obtained for an E_r process, given by Eq. (*7*) in Table I. However, in all the other previously mentioned mechanisms, the surface concentrations are dependent on time for the first pulse and subsequent potential pulses[4], and therefore the superposition principle cannot be applied and an analytical simple expression for the current corresponding to a given pulse *p*, I^p, cannot be expected.

By comparing Eq. (*1*) for the E_r process and Eq. (*25*) for the E_rC' mechanism, it is clear that the dependence of the current on the applied potential is identical in both mechanisms, and only appears through the surface concentrations. This behavior implies the following:

1) For simple pulse techniques, i.e. when the sums of Eqs (*25*) and (*1*) disappear and only one addend ($p = 1$) remains, the responses $I_{E_rC'}/E$ and I_{E_r}/E are given by

$$I_{E_rC'} = nFA\left(\frac{D_O}{\pi}\right)^{1/2} F_{E_rC'}(t)\,\frac{c_O^* - K_1 c_R^*}{1 + K_1} \tag{27}$$

and

$$I_{E_r} = nFA\left(\frac{D_O}{\pi}\right)^{1/2} F_{E_r}(t)\,\frac{c_O^* - K_1 c_R^*}{1 + K_1} \tag{28}$$

with $F_{E_rC'}(t)$ given by Eq. (*26*) and $F_{E_r}(t)$ given by Eq. (*3*) in Table I. Note that the only factor dependent on the applied potential for this first pulse has the same expression in both mechanisms, although for the E_rC' mechanism this factor can also be expressed as a function of the chemical equilibrium constant, $K_{eq} = c_R^*/c_O^* = k_2/k_1$, since

$$\frac{c_O^* - K_1 c_R^*}{1 + K_1} = \frac{(1 - K_1 K_{eq})(c_O^* + c_R^*)}{(1 - K_1)(1 + K_{eq})}\,. \tag{29}$$

This separability of the time–kinetic–geometric influence, $F_{E_rC'}(t)$, and the potential influence implies that for planar or spherical electrodes of any size, the $I_{E_rC'}$ response fulfils, for any value of time of the experiment and of the homogeneous rate constants, Eq. (*30*)

$$E = E^{0'} + \frac{RT}{nF} \ln \frac{I_{E_rC'}^{lc} - I_{E_rC'}}{I_{E_rC'} - I_{E_rC'}^{la}} \tag{30}$$

with $I_{E_rC'}$ given in Eq. (*27*), and the cathodic and anodic limit currents, $I^{lc}_{E_rC'}$ and $I^{la}_{E_rC'}$, are

$$I^{lc}_{E_rC'} = \frac{nFA(c^*_O + c^*_R)}{1 + K_{eq}} \left(\frac{D_O}{\pi} \right)^{1/2} F_{E_rC'}(t) \qquad (31)$$

and

$$I^{la}_{E_rC'} = \frac{-nFAK_{eq}(c^*_O + c^*_R)}{1 + K_{eq}} \left(\frac{D_O}{\pi} \right)^{1/2} F_{E_rC'}(t) \,. \qquad (32)$$

Therefore, it is clear that the *I*/*E* dependence for an E_rC' process (Eq. (*30*)) is identical to that shown for an E_r process[12,17].

2) In DPV technique two consecutive potentials, E^I and E^{II}, are applied to the working electrode, and the response is constructed by plotting the difference $\Delta I = I^{II} - I^I$ versus E^I (lit.[18–20]). In this technique, the influence of the first potential step in ΔI practically disappears due to $t_1 >> t_2$, and the expressions $\Delta I_{E_rC'}/E$ and $\Delta I_{E_r}/E$ show also the same dependence with the applied potential E^{II} ($E^{II} - E^I = \Delta E$ = constant). Both fulfil Eqs (*33*) and (*34*) for a spherical electrode of any size and for any value of the rate constants

$$\Delta I_{E_rC'} = nFA(c^*_O + c^*_R) \left(\frac{D_O}{\pi} \right)^{1/2} F_{E_rC'}(t_2) \left(\frac{1}{1 + K_2} - \frac{1}{1 + K_1} \right) \qquad (33)$$

and

$$\Delta I_{E_r} = nFA(c^*_O + c^*_R) \left(\frac{D_O}{\pi} \right)^{1/2} F_{E_r}(t_2) \left(\frac{1}{1 + K_2} - \frac{1}{1 + K_1} \right) \qquad (34)$$

in such a way that, although the current peaks are evidently different in both mechanisms, the potential peaks are in both cases $E_p = E^{0'} \pm |\Delta E|/2$ (lit.[21,22]), independently of the radius of the electrode.

3) In the particular case for CV technique, a comparison between Eqs (*25*) and (*26*), and Eqs (*1*) and (*3*) in Table I clearly shows that the behavior of the E_rC' process cannot be expected to be similar to that shown by an E_r outside the stationary state (i.e., for $(k_1 + k_2)t_{mp} < 2.0$). However, if we take into account that for an E_rC' process the influence of the electrode radius on $F_{E_rC'}(t_{mp})$, as in an E_r process, corresponds only to an addend independent of time, the terms dependent on r_0 in Eqs (*25*) and (*26*) cancel out in such a way that, taking into account Eq. (*9*), the dimensionless $\psi_{E_rC'}$, can be rewritten as[5]

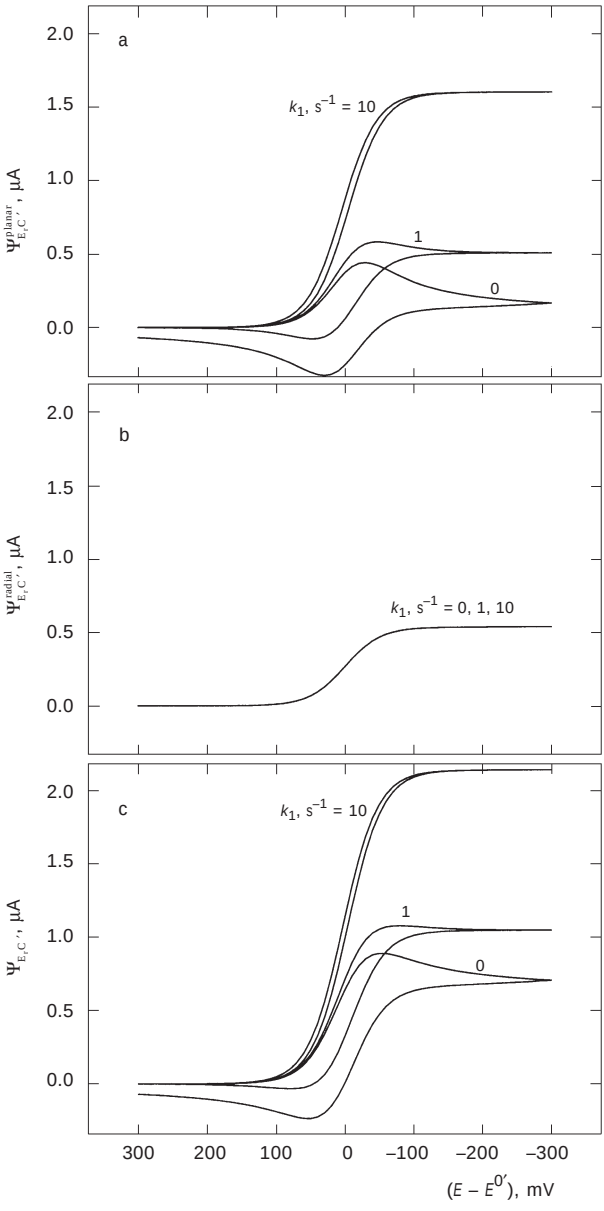

FIG. 6

Influence of the rate constant, k_1, on the dimensionless cyclic voltammograms obtained for a catalytic process. a Planar contribution, Eq. (*36*); b radial contribution, Eq. (*37*); c spherical electrode, Eq. (*35*). K_{eq} = 0. The values of k_1 (in s^{-1}) are given in the figure. Others conditions as in Fig. 1

$$\psi_{E_rC'} = \psi^{planar}_{E_rC'} + \psi^{radial}_{E_rC'} \quad , \tag{35}$$

where

$$\psi^{planar}_{E_rC'} = \frac{1}{(c^*_O + c^*_R)(\pi a)^{1/2}} \sum_{m=1}^{p} F^{planar}_{E_rC'}(t_{mp}) \left(c^{m-1}_{O,s} - c^{m}_{O,s} \right), \tag{36}$$

$$\psi^{radial}_{E_rC'} = \left(\frac{D}{a} \right)^{1/2} \frac{(c^*_O - K_p c^*_R)}{r_0 (c^*_O + c^*_R)(1 + K_p)} \tag{37}$$

and $F^{planar}_{E_rC'}(t_{mp})$ is given by Eq. (*26*) with $r_0 \to \infty$.

This result implies that there is a total analogy between the influence of the electrode radius on the response in an E_r and in an E_rC' process, i.e., the radial contribution depends only on the potential applied to the last pulse and is independent of sweep rate, *v*.

Figure 6 shows the effect of rate constants, $k_1 + k_2$, on the curves corresponding to planar (Fig. 6a) and radial contributions (Fig. 6b), as well as on the response in a conventional spherical electrode (Fig. 6c) for an E_rC' mechanism with $K_{eq} = 0$. Figure 6a shows that the planar contribution is the only one that depends on the kinetic constants of the chemical reaction, and so we can observe how the curve with $k_1 + k_2 = 10\ s^{-1}$ has already reached the kinetic steady state. Figure 6b corresponds to the radial contribution, which, being identical to that of an E_r process (cf. Figs 6b and 1b as well as Eqs (*15*) and (*37*)), is independent of kinetic parameters, as has been mentioned above. This contribution would be the only one observed when an ultramicrohemispherical electrode is used, since in this extreme case the microgeometrical steady state is reached[5] and therefore no kinetic influence is observed. Figure 6c shows the real CV response obtained in this conventional spherical electrode (Eq. (*35*)). This behavior implies that when the E_rC' mechanism is analyzed, it is not convenient to use spherical electrodes of small size since the kinetic influence decreases as the electrode radius decreases, independently of whether the kinetic steady state has been reached or not (see Fig. 6c).

The authors greatly appreciate the financial support provided by the Dirección General Científica y Técnica (Project No. BQU2003-04172), and by the Fundación Séneca (Project No. PB/53/FS/02). M. M. Moreno thanks Dirección General Científica y Técnica for the grant received.

REFERENCES

1. Molina A., Serna C., Camacho L.: *J. Electroanal. Chem.* **1995**, *394*, 1; and references therein.
2. Serna C., Molina A.: *J. Electroanal. Chem.* **1999**, *466*, 8; and references therein.
3. Serna C., Molina A., Moreno M. M., López-Tenés M.: *J. Electroanal. Chem.* **2003**, *546*, 97.
4. Molina A.: *J. Electroanal. Chem.* **1998**, *443*, 163.
5. Molina A., Serna C., González J.: *J. Electroanal. Chem.* **1998**, *454*, 15; and references therein.
6. Weidner J. W., Fedkiw P. S.: *Anal. Chem.* **1990**, *62*, 875.
7. Demortier A., Jehoulet C.: *J. Electroanal. Chem.* **1990**, *283*, 15.
8. Keightley A. M., Myland J. C., Oldham K. B., Symons P. G.: *J. Electroanal. Chem.* **1992**, *322*, 25.
9. Nicholson R. S., Shain I.: *Anal. Chem.* **1964**, *36*, 706.
10. Myland J. C., Oldham K. B.: *J. Electroanal. Chem.* **1983**, *153*, 43.
11. Reinmuth W. H.: *J. Am. Chem. Soc.* **1957**, *79*, 6358.
12. Galus Z.: *Fundamentals of Electrochemical Analysis*, 2nd ed. Ellis Horwood, Chichester 1994.
13. Paul H. J., Leddy J.: *Anal. Chem.* **1995**, *67*, 1661.
14. Zoski C. G., Bond A. M., Allison E. T., Oldham K. B.: *Anal. Chem.* **1990**, *62*, 37.
15. Molina A., Moreno M. M., Serna C., Camacho L.: *Electrochem. Commun.* **2001**, *3*, 324.
16. Krulic D., Fatouros N., Chevalet J.: *J. Electroanal. Chem.* **1990**, *287*, 215.
17. Bard A. J., Faulkner L. R.: *Electrochemical Methods*, 2nd ed. Wiley, New York 2000.
18. Birke R. L., Kim M.-H., Strassfeld M.: *Anal. Chem.* **1981**, *53*, 852.
19. Krulic D., Fatouros N., El Belamachi M. M.: *J. Electroanal. Chem.* **1995**, *385*, 33.
20. Kim M.-H., Yan L., Birke R. L., Czae M.-Z.: *Electroanalysis* **2003**, *15*, 1541.
21. Kim M.-H., Birke R. L.: *Anal. Chem.* **1983**, *55*, 522.
22. Serna C., Molina A., Martínez-Ortiz F., González J.: *J. Electroanal. Chem.* **1999**, *468*, 158.